Droplet shapes on structured substrates and conformal invariance

2001 J. Phys.: Condens. Matter 13 383

(http://iopscience.iop.org/0953-8984/13/3/303)

INSTITUTE OF PHYSICS PUBLISHING JOURNAL OF PHYSICS: CONDENSED MATTER

J. Phys.: Condens. Matter **13** (2001) 383–402 www.iop.org/Journals/cm PII: S0953-8984(01)16123-0

Droplet shapes on structured substrates and conformal invariance

A O Parry, E D Macdonald and C Rascón

Department of Mathematics, Imperial College, London SW7 2BZ, UK

Received 7 August 2000, in final form 20 October 2000

Abstract

We consider the finite-size scaling of equilibrium droplet shapes for fluid adsorption (at bulk two-phase coexistence) on heterogeneous substrates and also in wedge geometries in which only a finite domain Λ_A of the substrate is completely wet. For three-dimensional systems with short-ranged forces we use renormalization group ideas to establish that both the shape of the droplet height and the height–height correlations can be understood from the conformal invariance of an appropriate operator. This allows us to predict the explicit scaling form of the droplet height for a number of different domain shapes. For systems with long-ranged forces, conformal invariance is not obeyed but the droplet shape is still shown to exhibit strong scaling behaviour. We argue that droplet formation in heterogeneous wedge geometries also shows a number of different scaling regimes depending on the range of the forces. The conformal invariance of the wedge droplet shape for short-ranged forces is shown explicitly.

1. Introduction

There is currently much experimental and theoretical interest in the behaviour of fluid adsorption on structured substrates that are chemically heterogeneous [1–5] or that have a specific non-planar shape [6–10]. It is now appreciated that breaking the translational invariance along the substrate can lead to a number of highly interesting effects. These include surface phases that do not obey Young's contact angle equation [1–3], surface condensation-like phase transitions [4–6], non-trivial responses of the interface shape to substrate corrugation [7], geometry-dependent critical exponents for the growth of the adsorption at complete wetting [8] and even changes to the roughness exponent describing the fluctuations of the interface at filling transitions compared to wetting [9, 10]. In the present work we are concerned with the equilibrium shape of finite-size droplets on planar substrates and also in non-planar wedge geometries. We argue that within the grand canonical ensemble (without volume constraint) the droplet shape is characterized by universal scaling-like functions analogous to universal order-parameter profiles associated with finite-size effects in critical magnets and (binary) fluids [11, 12]. Our central new observation is that, for systems with short-ranged forces, the universal droplet shape may be understood from the conformal invariance of an appropriately

0953-8984/01/030383+20$30.00

defined surface operator. Indeed for such systems the conformal invariance may be proved explicitly using a straightforward renormalization group analysis. In this way we are able to make predictions for the explicit droplet shape on a number of pertinent heterogeneous substrates including those with striped and circular domains. The relevance of conformal invariance for the scaling behaviour of droplet shapes in wedge geometries is also discussed. We believe that our predictions can be tested in future numerical simulation studies of Ising models and may be open to experimental verification.

Our article is arranged as follows. In section 2 we discuss the case of droplet formation on planar substrates in (bulk) three-dimensional ($d = 3$) systems (i.e. a two-dimensional interface) concentrating on the case of systems with short-ranged forces (for which there may well be experimental systems) where the conformal invariance of the droplet shape and its correlations may be proved directly and used to understand the finite-size scaling behaviour. We finish this section by comparing this behaviour with previous predictions for systems with long-ranged forces and also a brief discussion of droplet formation for bulk dimension $d = 2$ where the result may also be related to the restrictions imposed by conformal invariance. In section 3 we identify the scaling functions describing the shape of droplets in heterogeneous wedge geometries exactly at the filling transition temperature for systems with both short-ranged and long-ranged dispersion forces. Again we find that the restrictions imposed by conformal invariance have relevance to droplet formation for short-ranged forces.

2. Droplets on planar substrates

To begin we discuss the case of droplet shapes on planar heterogeneous substrates. Consider a planar substrate in contact with a vapour phase which is at bulk liquid–vapour coexistence corresponding to saturation chemical potential $\mu = \mu_{sat}$. The substrate is chemically heterogeneous and consists of a finite-size simply connected domain Λ_A of substrate type A (which is assumed to extend over a region much larger than the bulk correlation length in all directions) which would be completely wetted by the liquid phase if the area was infinite, i.e. the local contact angle $\theta_A = 0$. Outside of the domain the substrate is of type B which is only partially wetted by the liquid phase at this temperature, so $\theta_B > 0$; see figure 1. These conditions induce the condensation of a large finite-size droplet over the domain Λ_A with the local height of the interface pinned to a finite value at the edges. An extreme example of this is if substrate B has contact angle $\theta_B = \pi$. This situation is realizable in experiments with water in which A is hydrophilic and B is hydrophobic say. Alternatively for Ising-like magnets one may envisage fixing the surface spins lying within Λ_A to be +1 and the spins outside to be

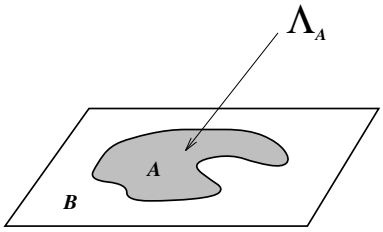

Figure 1. A schematic illustration of a heterogeneous planar substrate containing a finite-size domain of substrate type A which is completely wetted by liquid at bulk two-phase coexistence corresponding to local contact angle $\theta_A = 0$. Outside this domain the substrate is of type B and is only partially wetted, so $\theta_B > 0$. All length scales are considered larger than the bulk correlation length.

-1. As the area of the domain is increased so the equilibrium height of the droplet grows and becomes macroscopic. We are interested in the shape of the droplet for large domain sizes as this asymptotic limit is approached. In this limit the details of the wetting properties of B will not matter provided that they serve to pin the interface to a finite height at the domain boundary. Similarly we do not have to make any assumptions regarding the order of any wetting transition occurring for the substrate. The central question that we address here is how the shape of the domain Λ_A bounding the drop affects the equilibrium droplet shape. Note that there is no volume constraint imposed on the amount of liquid adsorbed on the domain, so the equilibrium shape of the interface necessarily has the same translational invariance as the underlying substrate binding potential (see [1, 2] for effects induced by volume constraint or equivalently by oversaturating the bulk vapour phase). The simplest possible starting point for discussing this problem which includes the effect of interfacial fluctuations and microscopic interactions is the interface Hamiltonian model [4, 5]

$$H[\ell] = \int \mathrm{d}\boldsymbol{x} \left\{ \frac{\Sigma}{2}(\nabla\ell)^2 + W(\ell; \boldsymbol{x}) \right\} \tag{1}$$

where $\ell(\boldsymbol{x})$ denotes the local interface height at position $\boldsymbol{x} = (x, y)$ along the substrate, Σ is the interfacial stiffness (equivalent to the tension for isotropic systems) of the unbinding fluid interface and $W(\ell; \boldsymbol{x})$ denotes a local position-dependent binding potential. The model is a valid description of the equilibrium droplet shape, and its fluctuations, at length scales much bigger than the bulk correlation length. For anisotropic lattice systems (such as the three-dimensional Ising model), the effective-Hamiltonian description is only valid above the roughening temperature T_r (with $T_r \approx 0.54\ T_c$ for a simple cubic lattice) and with an appropriate stiffness coefficient that accounts for the anisotropy of the surface tension. As the position $\boldsymbol{x}$ changes from outside to inside the domain so the local potential changes from being of type $W_B(\ell)$ to $W_A(\ell)$ as appropriate to the respective homogeneous B- and A-substrates. The crossover in $W(\ell; \boldsymbol{x})$ can be anticipated to occur over a finite distance λ_{AB} [4, 5] which itself depends on the range of the forces in the system. For short-ranged forces we anticipate that λ_{AB} is of order the bulk correlation length. This model also assumes that the interfacial gradient is small; otherwise the first term in (1) has to be replaced with the usual drumhead expression for the interfacial area. We will only be interested in the scaling properties of the droplet shape, however, which emerge when the gradient is small. For the model (1) it is straightforward to derive an exact Ward identity for the equilibrium interface position. Following the analysis of Mikheev and Weeks [13] (see also [14]) it is straightforward to show that

$$\Sigma\nabla^2\langle\ell\rangle = \langle\partial W(\ell; \boldsymbol{x})/\partial\ell\rangle \tag{2}$$

which relates the local effective force to the local interface curvature. Here $\langle\cdot\rangle$ denotes the usual ensemble average. Thus provided that we restrict our attention to the scaling limit of domain area $A_\Lambda \to \infty$ and positions $\boldsymbol{x}$ which are far from the domain edge, then the shape of the droplet is described by the solution of

$$\Sigma\nabla^2\langle\ell\rangle = \langle W_A'(\ell)\rangle \tag{3}$$

which serves as the starting point for our analysis. This scaling limit is analogous to that encountered in studies of universal order-parameter profiles in confined critical systems [11, 12]. To proceed we use the very well developed renormalization group (RG) theory of wetting [15–19] and replace the RHS of (3) with the derivative of an effective potential which is constructed on the basis of the linearized RG. In other words we rewrite (3) as

$$\Sigma\nabla^2\langle\ell\rangle = W_{eff}'(\langle\ell\rangle) \tag{4}$$

where the effective potential is derived by coarse graining the bare potential over the local roughness of the interfacial fluctuations. The net result (for dimension $d = 3$) is [15–19]

$$W_{eff}(\ell) = \int_{-\infty}^{\infty} \mathrm{d}t \; W(t) \frac{\mathrm{e}^{-(\ell-t)^2/2\xi_\perp^2}}{\sqrt{2\pi\xi_\perp^2}} \tag{5}$$

where

$$\xi_\perp = \sqrt{\frac{k_B T}{2\Sigma\pi} \ln \xi_\parallel}$$

is the local effective roughness and $\xi_\parallel$ is a transverse correlation length determined self-consistently by $\xi_\parallel^{-2} \propto W''_{eff}(\ell)$. This then is the desired field equation for the mean droplet height, the precise form of which depends on the range of the forces. Note that the existence of the effective potential implies that there exists a local free-energy functional $F[\ell]$ for the mean interfacial height (and its correlations) which is of the same form as (1) (at least within the desired region $\boldsymbol{x} \in \Lambda_A$) but with $W_A(\ell)$ replaced with $W_{eff}(\ell)$. The existence of a local free-energy functional for the droplet problem is directly related to the fact that the exponent analogous to the bulk correlation function exponent η is zero for wetting transitions. This has important simplifying consequences for the structure of correlations in the droplet which we will discuss later.

To continue we consider the cases of short-ranged and long-ranged forces separately.

2.1. Droplet shapes for short-ranged forces

For systems with short-ranged forces such as Ising and Landau–Ginzburg–Wilson models and also some experimentally accessible systems including polymers [20], some fluid mixtures [21] and superconductors [22], it is well understood [15–19] that the bare (unrenormalized) potential decays as $W_A(\ell) \sim A_s \mathrm{e}^{-\kappa\ell}$ with A_s an effective (positive) Hamaker constant and $\kappa \equiv 1/\xi_b$ the inverse bulk correlation length [23, 24]. We emphasize here that because the droplet shape reflects finite-size effects occurring at complete wetting, we only need account for the leading-order term in the decay of the binding potential. The renormalization of this is very well understood and gives rise to an effective potential which depends on the value of the wetting parameter $\omega = k_B T \kappa^2/(4\pi\Sigma)$. For values of $\omega < 2$ as are pertinent to fluids and Ising systems [23, 24] there is no need to consider the 'hard-wall' restriction $l > 0$ (which can only be treated approximately by the linear RG method) and the effective potential is $A_s \mathrm{e}^{-\tilde{\kappa}\ell}$ where $\tilde{\kappa} = \kappa/(1 + \omega/2)$ is a renormalized inverse length scale. The field equation for three-dimensional droplets with short-ranged forces is therefore

$$\Sigma \nabla^2 \langle \ell \rangle = -A_s \tilde{\kappa} \mathrm{e}^{-\tilde{\kappa}\langle \ell \rangle} \tag{6}$$

which we wish to solve for different shapes of the domain Λ_A. The central observation of this paper is that the above equation is conformally invariant with $\mathrm{e}^{-\tilde{\kappa}\langle \ell \rangle}$ playing the role of a primary operator with scaling dimension $x_b = 2$ [25]. The proof of this is straightforward, but tedious, and is presented in the appendix. Specifically, under a conformal map $z \to w$, where $w = u + \mathrm{i}v$ is an arbitrary analytic function of the complex variable $z = x + \mathrm{i}y$, the field equation (6) is invariant provided that we make the identification

$$\mathrm{e}^{-\tilde{\kappa}\langle \ell \rangle(u,v)} = |w'(z)|^{-2} \mathrm{e}^{-\tilde{\kappa}\langle \ell \rangle(x,y)}. \tag{7}$$

To exploit this result, consider the simplest example of a structured substrate consisting of two semi-infinite planes of type A, B which meet at the line $y = 0$ (see figure 2). From (6) it follows that $\mathrm{e}^{-\tilde{\kappa}\langle \ell \rangle}$ shows the scaling behaviour

$$\mathrm{e}^{-\tilde{\kappa}\langle \ell \rangle_{\infty/2}} = C y^{-2} \qquad \tilde{\kappa} y \gg 1 \tag{8}$$

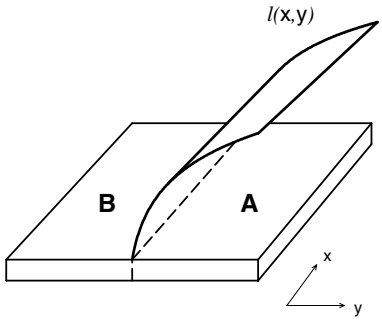

Figure 2. A heterogeneous substrate made from the union of two semi-infinite surfaces of type A and B. The mean interface height grows to infinity as we move further into the completely wet domain. For short-ranged forces the function $e^{-\tilde{\kappa}\langle\ell\rangle}$ has the scaling form $e^{-\tilde{\kappa}\langle\ell\rangle} \propto y^{-2}$ far from the $y = 0$ line.

so $\tilde{\kappa}\langle\ell\rangle_{\infty/2} \sim 2\ln(yC^{-1/2})$. Here $C = 2\Sigma/A\tilde{\kappa}^2$ is a non-universal constant. Following the analysis of Burkhardt and Eisenriegler [26] we now use some well known analytic functions to conformally map the semi-infinite system onto a number of pertinent finite-size domains and use (7) to identify the appropriate droplet shape. For example, the analytic functions

$$w = \frac{L}{\pi}\ln z \qquad w = \frac{L}{\pi}\cosh^{-1} z$$

map the half-plane onto the infinitely long strip $\{-\infty < u < \infty\} \cup \{0 < v < L\}$ and half-strip $\{u > 0\} \cup \{0 < v < L\}$ respectively. In this way we obtain the droplet shapes as

$$e^{-\tilde{\kappa}\langle\ell\rangle_{strip}} = C\left(\frac{L}{\pi}\sin\frac{\pi y}{L}\right)^{-2} \tag{9}$$

for $0 \ll \kappa y \ll \kappa L$ and

$$e^{-\tilde{\kappa}\langle\ell\rangle_{half-strip}} = C\left[\left(\frac{L}{\pi}\sinh\frac{\pi x}{L}\right)^{-2} + \left(\frac{L}{\pi}\sin\frac{\pi y}{L}\right)^{-2}\right] \tag{10}$$

for $0 \ll \kappa y \ll \kappa L$ and $\kappa x \gg 0$. Note that in writing these expressions we have changed our coordinate notation back to (x, y) rather than persisting with (u, v) (see figure 3).

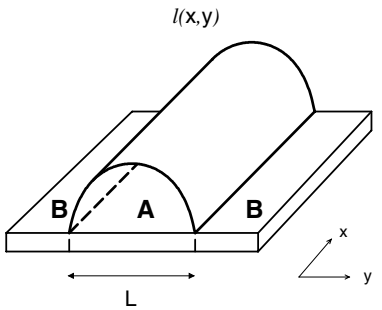

Figure 3. A schematic illustration of a droplet cross-section on a heterogeneous striped domain of finite width L. For short-ranged forces the analytic expression for the scaling of the droplet shape is obtained by conformally mapping the semi-infinite substrate shown in figure 2.

For circular domains of radius R the special conformal group can be used to obtain the desired droplet shape:

$$e^{-\tilde{\kappa}\langle\ell\rangle_{disc}} = C\left\{\frac{R}{2}\left[1-\left(\frac{r}{R}\right)^2\right]\right\}^{-2} \tag{11}$$

where r denotes the distance from the centre of the disc. This scaling expression is valid provided that $\kappa(R-r) \ll 1$. Note that the special conformal group can be used to map hyperplanes onto hyperspheres in arbitrary dimension, so we may anticipate that a result analogous to (11) may exist in other dimensions, in particular if the substrate (or unbinding interface) is effectively one dimensional. We shall return to this point later.

Equations (9) and (11) are our main predictions for droplet shapes in systems with short-ranged forces. We believe these to be the most relevant for future numerical and simulation studies and we finish this section with a discussion of them. Our first remark is that the droplet shape shows the same kind of finite-size scaling behaviour as predicted for order-parameter profiles in confined critical systems [11, 12]. Consider for example the result (9) for the strip domain. For large (but finite) distances from the droplet edge at the $y = 0$ line, the local height shows the 'distant-wall correction'

$$\tilde{\kappa}\langle\ell\rangle_{strip} = \tilde{\kappa}\langle\ell\rangle_{\infty/2} - \frac{\pi^2}{3}\left(\frac{y}{L}\right)^2 + \cdots \tag{12}$$

for $y/L \ll 1$. The power of L here reflects the two-dimensional character of the interface [11]. Secondly our results (9) and (11) for the droplet shape can be conveniently recast in scaling form by rewriting them in terms of the maximum height $\ell^{(m)}$ of the droplet occurring at the middle of the strip, disc domains. Thus for the strip we predict

$$\kappa(\langle\ell\rangle_{strip} - \ell^{(m)}_{strip}) = (2+\omega)\ln\sin\frac{\pi y}{L} \tag{13}$$

with $\ell^{(m)}_{strip} \propto \ln L$, whilst for the disc

$$\kappa(\langle\ell\rangle_{disc} - \ell^{(m)}_{disc}) = (2+\omega)\ln\left(1-\frac{r^2}{R^2}\right) \tag{14}$$

with $\ell^{(m)}_{disc} \propto \ln R$. Again we emphasize that the scaling function (13) is valid for $y \to \infty$, $L \to \infty$ with y/L arbitrary (and similarly for (14)). For finite L (or R) these predictions are appropriate provided that y (or r) is many bulk correlation lengths from the droplet edge. It is these expressions that we believe would be easiest to test in future simulation or experimental studies. Before we discuss the possibility of this, we mention here that in contrast to the case for studies of order-parameter profiles in confined critical magnets and fluids where the absolute value of the singular contribution to the mid-point magnetization (say) is very difficult to measure (because it vanishes as $L \to \infty$ or $R \to \infty$), the scaling of the droplet height is an obvious experimental observable. In particular, the above results make a precise prediction for the difference in maximum (mid-point) droplet height for the strip and disc domains. Specifically the difference in height of a droplet on an infinite strip of width L and that on a disc of identical diameter satisfies

$$\kappa(\ell^{(m)}_{strip} - \ell^{(m)}_{disc}) = (2+\omega)\ln\frac{4}{\pi} \tag{15}$$

which depends only on the value of the wetting parameter. It is remarkable how small this height difference is. In mean-field approximation which ignores fluctuation effects and has an effective value of $\omega = 0$, the numerical value of the RHS of (15) is only 0.4831, i.e. the droplet heights are different by less than half a bulk correlation length. Close to the bulk critical point

where ω approaches a universal value $\omega_c \simeq 0.77$ [23], this number increases to 0.67, but again the difference between the two heights is nearly negligible.

One of the first tests of these predictions would be to numerically study a mean-field Landau-like model of adsorption on heterogeneous walls. The influence of fluctuations on the droplet shape is rather small and the above results are valid even in the mean-field limit of $\omega = 0$. Beyond the mean-field level it would also be straightforward to consider Ising model simulation studies, above the roughening temperature, similar to those performed for wetting at homogeneous walls [27, 28]. We note that for this case it may well be that the appropriate value of $\tilde{\kappa}$ is altered by the coupling of interfacial fluctuations [29, 30]. This is certainly needed to quantitatively explain simulation studies [28] of (other) finite-size effects at complete wetting [31]. One obvious experimental constraint on these predictions is the role of gravity which both thins the height and dampens the fluctuations of the liquid–vapour interface. However, this effect will only become important if the strip width (say) is larger than the capillary length for gravity-damped interfacial modes. Using the value of the surface tension of water at room temperature, this implies that gravity may be neglected for strip widths or disc radii of less than a few micrometres.

2.2. Height fluctuations and correlations in the droplet

Next we turn our attention to the scaling properties of the height–height correlation function $S(\boldsymbol{x}_1, \boldsymbol{x}_2) = \langle \ell(\boldsymbol{x}_1)\ell(\boldsymbol{x}_2)\rangle - \langle \ell(\boldsymbol{x}_1)\rangle\langle \ell(\boldsymbol{x}_2)\rangle$. There are a number of ways of calculating this quantity, but following the treatment above we use the effective potential (5) to derive a renormalized Ornstein–Zernike (OZ) equation which for short-range forces reads

$$(-\Sigma\nabla^2_{x_1} + A_s\tilde{\kappa}^2 \mathrm{e}^{-\tilde{\kappa}\ell})S(\boldsymbol{x}_1, \boldsymbol{x}_2) = \delta(\boldsymbol{x}_2 - \boldsymbol{x}_1). \tag{16}$$

Here we point out the invariant properties of this equation as well its explicit solution for the semi-infinite and strip geometries. On making use of the covariant relation (7) it is straightforward to show that this equation is invariant under a conformal map $z \to w(z)$ with the correlation function transforming simply as

$$S(\boldsymbol{u}_1, \boldsymbol{u}_2) = S(\boldsymbol{x}_1, \boldsymbol{x}_2) \tag{17}$$

where we have adopted the notation $\boldsymbol{u}_1 = (u_1, v_1)$. The absence of an explicit scaling operator term in this result reflects the marginal logarithmic growth of the droplet height away from the boundary for systems with short-ranged heterogeneous forces. The transformation law for the height correlations is equivalent to the statement that the (connected) two-point correlator of the primary operator $\mathrm{e}^{-\kappa\ell}$ transforms as

$$\langle \mathrm{e}^{-\kappa\ell(\boldsymbol{u}_1)}\mathrm{e}^{-\kappa\ell(\boldsymbol{u}_2)}\rangle_{G'} = |w'(z_1)|^{-2}|w'(z_2)|^{-2}\langle \mathrm{e}^{-\kappa\ell(\boldsymbol{x}_1)}\mathrm{e}^{-\kappa\ell(\boldsymbol{x}_2)}\rangle_G \tag{18}$$

where the subscripts G' and G refer to ensemble averages with respect to the different geometries under the conformal transformation. That (17) and (18) are equivalent again is due to the existence of a renormalized local binding potential which accounts for fluctuation effects. Having established that the height–height correlation function transforms conformally, it immediately follows from the analysis of Cardy [32] that on the semi-infinite planar surface (figure 2) the two-point function depends only on a single variable such that

$$S_{\infty/2}(\boldsymbol{x}_1, \boldsymbol{x}_2) = \Phi\left(\frac{(x_1 - x_2)^2 + y_1^2 + y_2^2}{2y_1 y_2}\right). \tag{19}$$

The scaling function is then determined by substituting this result into the OZ equation (16) with $\mathrm{e}^{-\tilde{\kappa}\ell}$ given by (7). We find that $\Phi(t)$ satisfies

$$(t^2 - 1)\Phi'' + 2t\Phi' - 2\Phi = 0 \tag{20}$$

from which we can easily determine the important asymptotic behaviour. At short distances $\boldsymbol{x}_1 \to \boldsymbol{x}_2$ corresponding to $t \to 1$, it follows that $\Phi \sim \ln(t-1)$, implying that the local roughness $\xi_\perp \sim \sqrt{\ln y}$ precisely as expected for interfacial fluctuations at the marginal dimension $d = 3$. On the other hand, in the limit of large transverse separations $|\boldsymbol{x}_2 - \boldsymbol{x}_1| \to \infty$ corresponding to $t \to \infty$, it follows from (13) that $\Phi \sim t^{-2}$, which identifies the surface scaling exponent $\eta_\parallel = 4$ [32, 33]. It is this limit of the scaling function which is required in order to understand the asymptotic decay of correlations in the infinite finite-width strip geometry. Using the mapping discussed above, it immediately follows from (12) that the height–height correlation function decays as

$$S_{strip}(\boldsymbol{x}_1, \boldsymbol{x}_2) \simeq \sin^2\left(\frac{\pi y_1}{L}\right) \sin^2\left(\frac{\pi y_2}{L}\right) \mathrm{e}^{-2\pi |x_2 - x_1|/L} \tag{21}$$

for $|x_2 - x_1| \gg L$. In writing this expression we have again chosen to use the original coordinate notation rather than (u, v). The above expression identifies the universal finite-size droplet correlation length $\xi_\parallel = L/2\pi$. This identification is consistent with the amplitude–exponent relation $L/\xi_\parallel = 2/\pi\eta_\parallel$ [11].

We note here that the same result for $S(\boldsymbol{x}_1, \boldsymbol{x}_2)$ in the strip follows from explicit solution of the OZ equation (11) using the derived expression for the droplet height (8). This can be written as a spectral expansion

$$S_{strip}(\boldsymbol{x}_1, \boldsymbol{x}_2) = \sum_{n=0}^{\infty} \psi_n^*(y_1)\psi_n(y_2)\mathrm{e}^{-E_n|x_2 - x_1|} \tag{22}$$

with eigenvalues and eigenvectors determined from solution of

$$-\psi_n'' + 2\left(\frac{L}{\pi}\sin\frac{\pi y}{L}\right)^{-2}\psi_n = E_n^2\psi_n \tag{23}$$

subject to $\psi_n(0) = \psi_n(L) = 0$ and the orthonormality condition

$$2\Sigma \int_0^L \mathrm{d}y\ \psi_n^*(y)\psi_m(y) = \delta_{nm}E_n^{-1}. \tag{24}$$

The solution to (23) is found using standard methods. For the eigenvalue spectrum we find $E_n = (n+2)\pi/L$ (with $n = 0, 1, 2, \ldots$) whilst the eigenvectors are

$$\psi_n(x) = N_n \sin^2\left(\frac{\pi x}{L}\right) F\left[-\frac{n}{2}, 2 + \frac{n}{2}, \frac{1}{2}; \cos^2\frac{\pi x}{L}\right] \tag{25}$$

for $n = 0, 2, 4, \ldots$ and

$$\psi_n(x) = N_n \sin^2\left(\frac{\pi x}{L}\right) \cos\frac{\pi x}{L} F\left[\frac{1}{2} - \frac{n}{2}, \frac{5}{2} + \frac{n}{2}, \frac{3}{2}; \cos^2\frac{\pi x}{L}\right] \tag{26}$$

for $n = 1, 3, 5, \ldots$. Here $F[\alpha, \beta, \gamma; x]$ denotes the usual hypergeometric function. We note here that the fact that the exact result for $S(\boldsymbol{x}_1, \boldsymbol{x}_1)$ in the strip geometry obtained by conformally mapping the semi-infinite correlation function also follows from the solution to a local field equation (16) is intimately related to the existence of a local effective free-energy functional for complete wetting, which in turn reflects the fact that there is no exponent analogous to the η occurring for bulk critical systems. In studies of finite-size effects in strip (and other) geometries occurring at bulk criticality (for which $\eta \neq 0$), local field equations for the pair correlation function derived from approximate local functional models [34] do not capture all the necessary scaling features required by conformal invariance (although they are surprisingly accurate and highly reliable for certain quantities [35]).

As a final remark concerning height–height correlations in the strip geometry, we note that the existence of a renormalized local binding potential also implies that the correlations in

the strip satisfy the algebra of correlations discussed by Parry and Swain [36] in the somewhat different context of magnetization functionals. Defining the Fourier transform of the correlation function $\tilde{S}(y_1, y_2; \boldsymbol{q})$ by

$$\tilde{S}(y_1, y_2; \boldsymbol{q}) = \int \mathrm{d}\boldsymbol{x}_{21}\, \mathrm{e}^{-\mathrm{i}\boldsymbol{q}\cdot(\boldsymbol{x}_2-\boldsymbol{x}_1)} S(\boldsymbol{x}_1, \boldsymbol{x}_2) \tag{27}$$

and in particular denoting the zeroth moment by $\tilde{S}_0(y_1, y_2) = \tilde{S}(y_1, y_2; 0)$, it follows from the local character of the renormalized effective free-energy functional that for any ordered points $0 \leqslant y_1 \leqslant y_2 \leqslant y_3 \leqslant L$, the correlations satisfy

$$\tilde{S}(y_1, y_2; \boldsymbol{q})\tilde{S}(y_2, y_3; \boldsymbol{q}) = \tilde{S}(y_1, y_3; \boldsymbol{q})\tilde{S}(y_2, y_2; \boldsymbol{q}) \tag{28}$$

and

$$\begin{aligned}\left(\frac{\tilde{S}_0(y_1, y_3)}{\ell'(y_1)\ell'(y_3)} - \frac{\tilde{S}_0(y_1, y_2)}{\ell'(y_1)\ell'(y_2)}\right)\left(\frac{\tilde{S}_0(y_1, y_3)}{\ell'(y_1)\ell'(y_3)} - \frac{\tilde{S}_0(y_2, y_3)}{\ell'(y_2)\ell'(y_3)}\right) \\ = \left(\frac{\tilde{S}_0(y_1, y_1)}{\ell'(y_1)\ell'(y_1)} - \frac{\tilde{S}_0(y_1, y_2)}{\ell'(y_1)\ell'(y_2)}\right)\left(\frac{\tilde{S}_0(y_3, y_3)}{\ell'(y_3)\ell'(y_3)} - \frac{\tilde{S}_0(y_2, y_3)}{\ell'(y_2)\ell'(y_3)}\right)\end{aligned} \tag{29}$$

where $\ell'(y)$ denotes the derivative of the equilibrium height profile given by (9). These relations severely restrict the possible form of $\tilde{S}_0(y_1, y_2)$. In particular they imply that the dimensionless quantity

$$\sigma(y_1, y_2) \equiv \frac{\tilde{S}_0(y_1, y_2)}{\ell'(y_1)\ell'(y_2)} \frac{1}{k_B T} \frac{\partial^2 \Delta F}{\partial L^2} \tag{30}$$

where $\Delta F(L)$ denotes the excess or finite-size contribution to the droplet free energy, satisfies

$$\sigma(y_1, y_2) = (1 - \sqrt{1 - \sigma(y_1, y_1)})(1 \pm \sqrt{1 - \sigma(y_2, y_2)}) \qquad y_1 < \frac{L}{2} \tag{31}$$

and the $\pm$ signs refer to whether y_1 and y_2 are on the same/opposite side of the mid-line at $y = L/2$. We emphasize here that the results (28)–(31) are valid for any choice of effective binding potential (5) and are not specific to the exponential form for systems with short-ranged forces. The central prediction (31) of the correlation function algebra relates the correlation function structure within the droplet to the excess free energy $\Delta F(L)$. For the droplet with short-ranged forces, $\Delta F(L)$ is readily calculated using the appropriate effective free-energy functional. We find

$$\Delta F(L) = \frac{\pi}{8\omega}(2 + \omega)^2 L^{-1}. \tag{32}$$

Again the width dependence of this quantity is precisely in accord with dimensional (hyper-scaling) ideas for confinement in critical systems [12]. Note that the (Casimir) amplitude here is strongly non-universal and depends on the value of ω. This is in contrast to finite-size effects at bulk criticality (in Ising systems for example) where the amplitude of $\Delta F(L)$ is universal and related to the central charge [12] characterizing the bulk universality class. The derivative of the free energy determines the force of solvation between the edges of the strip, which might be measurable in force-balance experiments if the width L of the droplet can be controlled externally.

2.3. Droplets shapes and correlations with long-ranged forces

In the last section we explicitly showed and exploited the conformal invariance of the droplet shape and its correlations for systems with short-ranged forces. Whilst some examples of such systems may well be found in the laboratory, most solid–fluid and fluid–fluid systems will be

dominated by dispersion forces for which the bare binding potential (of the completely wet A-region) decays like $W_A \sim A_l \ell^{-2}$ where again A_l is an effective (positive) Hamaker constant. It is well understood [37] that this potential is not changed by fluctuations for $d = 3$, so the field equation for the droplet shape is simply

$$\Sigma \nabla^2 \langle \ell \rangle = -2A_l \langle \ell \rangle^{-3}. \tag{33}$$

This equation is certainly not invariant under the same kind of conformal mapping as is valid for systems with short-ranged forces consistent with general expectations of conditions for conformal invariance. In order to investigate the possible scaling properties of different finite-size droplet shapes it is therefore necessary to solve (33) explicitly for different domains. Here we concentrate on the infinite strip and disc domains only. The strip geometry has been discussed by Bauer and Dietrich [5] who point out that the droplet shows scaling behaviour with

$$\langle \ell \rangle_{strip} = 2\ell^{(m)}_{strip} \sqrt{\frac{y}{L}\left(1 - \frac{y}{L}\right)} \qquad 0 < y < L \tag{34}$$

where $\ell^{(m)}_{strip} \propto L^{1/2}$ is the maximum (mid-point) height of the drop. Thus whilst there is no conformal invariance for the droplet with dispersion forces, there is still a strong degree of scaling in this system. Indeed the scaling of the height profile for long-ranged forces is stronger than that predicted for short-ranged forces as can be seen from comparison with (13). Notice that near the edges of the droplet the interface height behaves as $\ell_{strip} \sim y^{1/2}$ (for $y/L \to 0$ say) where the power law here can be identified with the ratio of complete wetting exponents $\beta_{co}/\nu_{\|}$ where β_{co} is the adsorption critical exponent and $\nu_{\|}$ is the transverse correlation length critical exponents. For systems with dispersion forces, recall that $\beta_{co} = 1/3$ and $\nu_{\|} = 2/3$ consistent with the explicit shape dependence give above (see for example [18]).

Correlations along the droplet show a similar scaling structure. From the OZ equation

$$\left[-\Sigma \nabla^2_{\boldsymbol{x}_1} + W''_{eff}(\langle \ell \rangle)\right] S(\boldsymbol{x}_1, \boldsymbol{x}_2) = \delta(\boldsymbol{x}_2 - \boldsymbol{x}_1) \tag{35}$$

it follows from the spectral analysis given earlier that $S(\boldsymbol{x}_1, \boldsymbol{x}_2)$ decays asymptotically as

$$S(\boldsymbol{x}_1, \boldsymbol{x}_2) \sim \psi_0(y_1)\psi_0(y_2) \mathrm{e}^{-E_0|x_2 - x_1|} \qquad \frac{|x_2 - x_1|}{L} \to \infty \tag{36}$$

where ψ_0 and E_0 are found from numerical solution of the eigenvalue problem

$$-\psi_0'' + \frac{3L^2}{4y^2(L^2 - y^2)}\psi_0 = E_0^2 \psi_0 \tag{37}$$

with $\psi_0(0) = \psi_0(L) = 0$. In this way we find that the finite-size correlation length characterizing height fluctuations along the droplet satisfies $L/\xi_{\|} \simeq 5.25$, which is universal in the sense that it does not depend on the value of the surface tension or Hamaker constant. Interestingly, the ratio is smaller than that derived earlier for short-ranged forces, in keeping with general expectations about the influence of long-ranged forces on the range of correlations.

For droplet shapes on circular domains of radius R, it follows from (33) that the equilibrium height profile also has a scaling form $\langle \ell \rangle_{disc} = \ell^{(m)}_{disc} \Lambda(r/R)$ where $\ell^{(m)}_{disc} \propto R^{1/2}$ is the mid-point height and $\Lambda(\xi)$ is a scaling function satisfying $\Lambda(0) = 1$ and $\Lambda(1) = 0$ which can be determined numerically. Following our earlier treatment of droplets with short-ranged forces, it is interesting to compare the maximum droplet height for a circular domain of diameter $2R = L$ with the corresponding droplet height for a strip geometry. Because there is a stronger manifestation of scaling for systems with long-ranged forces, the comparison takes the form of a ratio $\ell^{(m)}_{strip}/\ell^{(m)}_{disc} \simeq 1.03$ rather than a difference as for short-ranged forces (15). The influence of the domain shape on the droplet adsorption is therefore stronger for systems

with dispersion forces even though the scaled heights are again very close to each other. A comparison of the corresponding droplet shapes is shown in figure 4 for strips and discs with long-ranged forces.

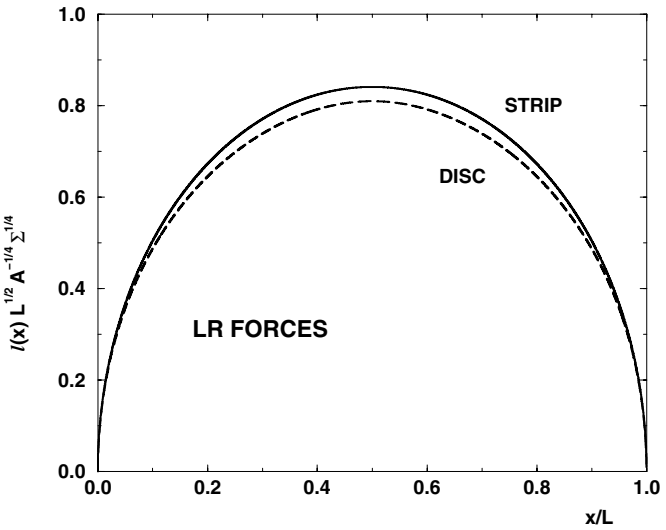

Figure 4. Comparison of the scaled interfacial height profiles for the strip and disc geometries for systems with dispersion forces. The disc radius R is equal to the strip half-width. The height is measured in appropriate dimensionless units whilst the scaling variable x/L denotes both the scaled distance across the strip and the radial distance across the disc.

2.4. Droplet shapes in 1 + 1 *dimensions*

To end this section and motivate out treatment of droplet shapes in three-dimensional wedges, we remark here that the scaling form of the droplet height for adsorption on a one-dimensional heterogeneous substrate also shows scaling behaviour that can be understand using conformal invariance. To be concrete, consider a two-dimensional semi-infinite Ising model at temperature T (less than the bulk critical value T_c) and in zero magnetic field $H = 0^-$ (so that the bulk phase has negative magnetization). The surface spins on the $y = 0$ line are all fixed to be down except along the line between $x = 0$ and $+L$ where they are all up. This is the two-dimensional analogue of the striped heterogeneous surface and the circular domain considered above. These boundary conditions induce the formation of a droplet of local equilibrium height $\ell(x)$ which is pinned to the wall at the end-points $x = 0$ and $x = L$. In the limit of $L \to \infty$ the droplet becomes macroscopic in size and we can anticipate that the shape shows scaling behaviour. The interfacial model for this problem is

$$H[\ell] = \int_0^L \mathrm{d}x \, \left\{ \frac{\Sigma}{2} \left(\frac{\mathrm{d}\ell}{\mathrm{d}x} \right)^2 + W(\ell) \right\} \tag{38}$$

where the binding potential $W(\ell)$ may be simply approximated by an infinite hard-wall potential $W(\ell) = 0$ for $\ell > 0$ and $W(\ell) = \infty$ otherwise, which simply restricts the interface to the $l > 0$ region. The reason for this is that for $d = 2$ the entropic repulsion of the interface from the hard wall dominates over any short-ranged interaction (for complete wetting problems) [17–19]. This problem has been considered by Burkhardt [38] using continuum transfer-matrix

techniques with the scaling behaviour of $\ell(x)$ explicitly calculated to be

$$\langle \ell(x) \rangle = 2\ell_0^{(m)} \sqrt{\frac{x}{L}\left(1 - \frac{x}{L}\right)} \tag{39}$$

where $\ell_0^{(m)} \propto L^{1/2}$ denotes the mid-point droplet height. Note that this expression is identical to that derived above for (2 + 1)-dimensional systems with dispersion forces. Here we make two relevant remarks concerning this transfer-matrix result:

(i) The scaling of $\langle \ell(x) \rangle$ in two dimensions is precisely what one would expect due to the entropic repulsion from the hard wall. The droplet shape reflects interfacial finite-size effects in the weak-fluctuation (WFL) regime [17, 18] which can be quantitatively understood using an effective potential which decays as $W_{FL} \propto A_{FL}\ell^{-2}$. Using this form for the effective potential, the field equation (4) reduces to

$$\Sigma \langle \ell \rangle'' = -2A_{FL}\langle \ell \rangle^{-3} \tag{40}$$

which is trivially integrated to recover the exact transfer-matrix result (39).

(ii) The scaling of $\langle \ell(x) \rangle$ is also in accord with the predictions of conformal invariance for (non-trivial) one-dimensional field theories. In general, phase transitions do not occur in (classical) one-dimensional systems unless either extremely long-ranged forces are present or the order parameter is allowed to diverge. The study of droplet shapes in (1 + 1)-dimensional systems is therefore an interesting test of the ideas of conformal invariance in this dimension. To see this first consider the limit of $L \to \infty$. Then, far from the pinned edge of the droplet, the height $\ell(x)$ scales as

$$\langle \ell(x) \rangle \sim Dx^{\zeta} \qquad \kappa x \gg 1 \tag{41}$$

where $\zeta = 1/2$ is the usual interfacial wandering exponent for the one-dimensional interface [18, 19]. This behaviour is consistent with the homogeneous rescaling $x \to x/b$ under which $\langle \ell(x) \rangle$ transforms as

$$\langle \ell(x/b) \rangle = b^{-\zeta} \langle \ell(x) \rangle. \tag{42}$$

It is natural to generalize this statement to non-uniform rescalings corresponding to the one-dimensional limit of special conformal mappings, such that

$$\langle \ell \rangle_{G'} = \left(\frac{\mathrm{d}x'}{\mathrm{d}x}\right)^{\zeta} \langle \ell(x) \rangle_G \tag{43}$$

where as before G' and G refer to ensemble averages with respect to the old and new geometries respectively. The allowed class of transformations that combines uniform rescalings, translations and inversions is therefore of the form

$$x' = \frac{a + bx}{c + dx} \tag{44}$$

with $ad - bc \neq 0$ (since otherwise the scale factor vanishes). This transformation maps the semi-infinite line to a line of finite length. Choosing a, b, c and d such that $0 < x' < L$ we find

$$\langle \ell(x') \rangle = \ell_0^{(m)} 4^{\zeta} \left[\frac{x'}{L}\left(1 - \frac{x'}{L}\right)\right]^{\zeta} \tag{45}$$

which is of course identical to the transfer-matrix result (39) provided that we identify the correct value of the wandering exponent. Note that if we write this expression in terms of the distance $x'' = x' - L/2$ from the centre of the strip, then the position dependence of the scaling function is basically identical to that observed for circular domains for $d = 3$ but

with a different value of ζ (see (14)). This is because the scaling function for the height of radially symmetric drops on heterogeneous substrates (with short-ranged forces) in arbitrary dimension can be obtained by the application of the special conformal mapping analogous to (44).

To finish this section we emphasize here that the only ingredient in deriving the prediction (45) is the assumption of covariance under the special conformal mapping (44). The finite-size droplet in 1 + 1 dimensions is a specific example of this one-dimensional prediction of conformal invariance for a problem in which $\zeta = 1/2$. In the next section we shall show that (45) has application for a second example of interfacial phenomena.

3. Droplet shapes in three-dimensional wedge geometries

The calculations presented in section 2 assume that the substrate is heterogeneous but still planar. However, recently it has been shown that chemically homogeneous but non-planar substrates in the shape of wedge geometries exhibit filling or wedge-wetting transitions which are characterized by very strong interfacial fluctuations belonging to universality classes and fluctuation regimes quite distinct from those occurring for wetting at a planar wall [10]. The purpose of this section is to investigate the scaling of droplet shapes in wedge geometries. Before we study these finite-size effects we briefly review the phenomenology of filling transitions and the recently developed fluctuation theory for them based on analysis of a novel interfacial Hamiltonian [10]. This model will form the starting point for our study of droplet shapes in wedges.

3.1. Filling transitions and effective-Hamiltonian theory

Consider a wedge formed by the union of two walls at angles $\pm\alpha$ to the horizontal. The wedge is supposed to be in contact with a bulk vapour phase at saturation chemical potential $\mu = \mu_{sat}(T)^-$ and is at a temperature T less than the wetting transition temperature T_w of the planar wall–vapour interface. Thermodynamic arguments [39–41] dictate that the wedge is completely filled with liquid at a temperature T_F satisfying

$$\theta(T_F) = \alpha \tag{46}$$

and $\theta(T)$ denotes the contact angle of the liquid drop on the planar substrate. This thermodynamic prediction is confirmed by specific model calculations which include the influence of intermolecular interactions and fluctuation effects [9, 10]. The filling transition occurring as $T \to T_F$ may be first or second order [42] corresponding to the discontinuous or continuous divergence of the interfacial height ℓ_0 as measured from the bottom of the wedge. Importantly, even substrates that exhibit first-order wetting transitions can exhibit continuous filling transitions [10], so the experimental observation of critical (continuous) filling is a realistic possibility. In addition to the divergence of ℓ_0 as $T \to T_F^-$, the filling transition is characterized by the divergence of distinct correlation lengths along ($\xi_y \sim (T_F - T)^{-\nu_y}$) and across ($\xi_x \sim (T_F - T)^{-\nu_x}$) the wedge, as well as the roughness $\xi_\perp$ of the unbinding interface (see figure 5) [10].

The mean-field critical behaviour has been examined in detail [10] from analysis of the non-planar version of the standard interfacial Hamiltonian (valid for small α) given by

$$H[l] = \int \mathrm{d}\boldsymbol{x} \left\{ \frac{\Sigma}{2}(\nabla\ell)^2 + W(\ell - \alpha|x|) \right\} \tag{47}$$

where $\ell(\boldsymbol{x})$ is the local height of the interface as measured from the plane and $W(l)$ is the usual binding potential. The mean-field critical exponents for filling are determined only by

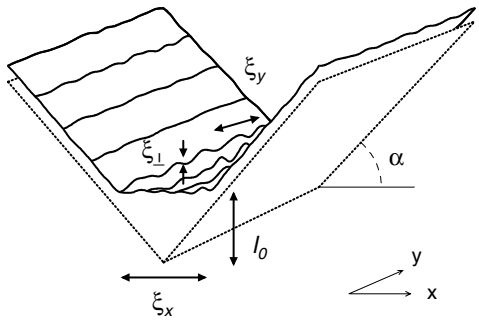

Figure 5. A section of an interfacial configuration occurring in a wedge geometry. As the critical filling transition temperature T_W is approached, the mean mid-point height ℓ_0^{max}, roughness $\xi_\perp$ and anisotropic correlation lengths ξ_x, ξ_y diverge continuously. The extreme anisotropy of the fluctuations means that the transition is quasi-one dimensional.

the leading-order decay term in $W(\ell)$. Writing this as $W(\ell) = -A_l \ell^{-p}$ (so that $p = 2$ corresponds to non-retarded dispersion forces), the critical exponents are given by

$$\beta_0 = \frac{1}{p} \qquad \nu_x = \frac{1}{p} \qquad \nu_y = \frac{1}{2} + \frac{1}{p} \qquad \nu_\perp = \frac{1}{4}. \tag{48}$$

Notice the remarkable universal value of the roughness critical exponent. Analysis of the height–height correlations at filling shows that fluctuations across the wedge are highly localized to the filled region with the local height $\ell(\boldsymbol{x})$ at position y along the wedge fluctuating coherently; i.e. the effective stiffness across the filled portion of the wedge is infinite. In this sense, fluctuations across the wedge are trivial, which can be seen in the explicit values of the critical exponents since $\beta_0 = \nu_x$ for all values of p. On the other hand, correlations along the wedge are characterized by a soft mode and completely dominate the fluctuation behaviour. On the basis of this, Parry, Rascón and Wood [10] have argued that the fluctuation theory of three-dimensional filling transitions can be understood using the effective one-dimensional model

$$H_F[\ell_0] = \int \mathrm{d}y \, \left\{ \frac{\Sigma \ell_0}{\alpha} \left(\frac{\mathrm{d}\ell_0}{\mathrm{d}y} \right)^2 + V(\ell_0) \right\} \tag{49}$$

where $\ell_0(y) = \ell(0, y)$ is the local height of the interface at the centre of the wedge. This model is based on the assumption that only fluctuations along the wedge contribute to the asymptotic critical behaviour (see figure 6).

This effective model is only presumed correct for the soft-mode fluctuations in the y-direction which determine the asymptotic critical behaviour. The model is not valid for wavevectors $Q > Q_{max} \simeq 1/\xi_x$. At this scale the full 2D model (47) has to be used. Notice that the coefficient of the bending term is proportional to the local height of the filled region (quite unlike the stiffness term for planar fluid interfaces), reflecting the fact that a local increase in the height also increases the width of the filled region in the x-direction. The direct filling potential appearing in (49) is found to be

$$V(\ell_0) = \frac{\Sigma}{\alpha}(\theta^2 - \alpha^2)\ell_0 + A_F \ell_0^{1-p} + \cdots \tag{50}$$

the minimum of which identifies the mean-field ℓ_0. This filling Hamiltonian can be studied exactly using transfer-matrix techniques, yielding a complete classification of the possible

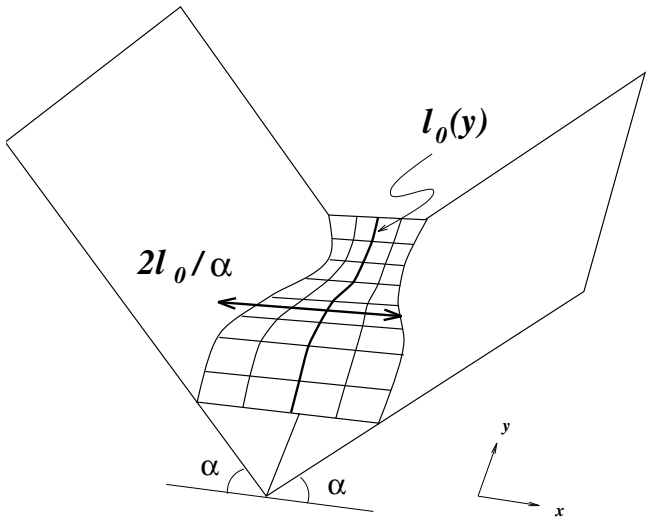

Figure 6. A schematic illustration of an interfacial configuration in the wedge geometry viewed on a scale larger than ξ_x. Fluctuations in the local height across the wedge have disappeared, leaving only the quasi-one-dimensional undulations of the mid-point height along the system.

critical behaviours. For $p < 4$ mean-field theory is valid, whilst for $p > 4$ the critical behaviour is universal with critical exponents given by

$$\beta_0 = \frac{1}{4} \qquad \nu_x = \frac{1}{4} \qquad \nu_y = \frac{3}{4} \qquad \nu_\perp = \frac{1}{4}. \tag{51}$$

Notice that in the fluctuation-dominated regime, $\beta_0 = \nu_\perp$, so there are regular excursions of the interface to the wedge bottom. The existence of two fluctuation regimes for critical filling can be understood using arguments analogous to the well developed scaling theory of wetting [17–20]. To see this, we suppose that the influence of fluctuations at critical filling can be understood using an effective potential

$$V_{eff}(\ell_0) = V(\ell_0) + V_{FL}(\ell_0) \tag{52}$$

which accounts for fluctuation effects by adding to the direct potential a term arising from the entropic repulsion from the wedge bottom. The fluctuation term can be estimated from the form of the bending energy contribution to (49) as $V_{FL}(\ell_0) \simeq \ell_0^3 \xi_y^{-2}$ and hence

$$V_{FL}(\ell_0) \simeq \ell_0^{3-2/\zeta} \tag{53}$$

where ζ is the wandering exponent for filling transitions which relates the roughness $\xi_\perp \sim \xi_y^\zeta$ and soft-mode correlation length ξ_y. The value $\zeta = 1/3$ can be read directly either from the transfer-matrix results (51) or equivalently from the scale invariance of the free filling Hamiltonian

$$H_0 = \int \mathrm{d}y \, \frac{\Sigma \ell_0}{\alpha} \left(\frac{\mathrm{d}\ell_y}{\mathrm{d}y} \right)^2$$

under the scale transformations $y \to y/b$ and $\ell \to \ell/b^\zeta$. The net result of this is an effective filling potential of the form

$$V_{eff}(\ell_0) = V(\ell_0) + D\ell_0^{-3} \tag{54}$$

which is minimized to find the equilibrium film thickness ℓ_0. Thus we find a mean-field or fluctuation-dominated regime depending on whether the entropic repulsion or direct algebraic

term $A_F \ell^{1-p}$ is the dominant correction to the linear term. Unlike critical wetting for which there are three fluctuation regimes, critical filling only has two since the linear term in the direct binding potential is always relevant. In this sense, fluctuation effects at three-dimensional critical filling are rather similar to those occurring at two-dimensional complete wetting [17–20, 37].

3.2. Finite-size droplets in heterogeneous wedge geometries

We are now in a position to consider the finite-size scaling of droplet shapes in heterogeneous wedge geometries formed by sandwiching a finite-length wedge of substrate type A between two wedges of type B (see figure 7).

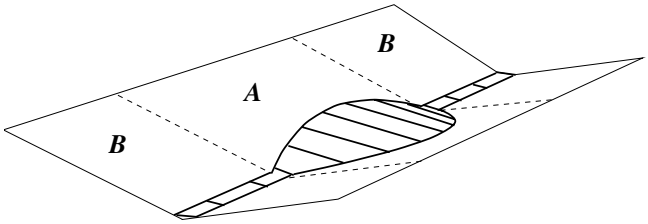

Figure 7. A heterogeneous wedge containing a finite-size region A which satisfies the local filling condition $\theta_A(T_F) = \alpha$. Outside this strip, in the region B, the wedge is only partially filled.

Following our earlier treatment of heterogeneous planar substrates, we suppose that exactly at the saturation chemical potential $\mu = \mu_{sat}(T)^-$ the filling height on the B-wedge is finite but that an infinite domain of A-wedge would be completely filled. This geometry induces the condensation of a large droplet of liquid over the A-region with the interface height pinned to finite values at the end-points (taken to be $y = 0$ and $y = L$). As before, there is no volume constraint on the amount of liquid adsorbed, with the result that the maximum height of the droplet $\ell_0^{max} \to \infty$ as $L \to \infty$ and we can anticipate scaling behaviour for the position dependence of the equilibrium profile $\langle \ell_0(y) \rangle$. The details of the partial filling of the B-region are not important for the scaling structure of the droplet shape and there are a number of specific ways of inducing the pinning. For example, if the contact angle of the liquid drop on the planar B-substrate $\theta_B > \pi/2$, then the associated wedge is never filled (by liquid) for any temperature. If $\theta_B < \pi/2$, then one has to choose substrate A such that $\theta_A < \theta_B$ so that the A-wedge fills before the B-wedge. We now distinguish between two distinct manifestations of scaling for the finite-size droplet shape:

(A) *Droplet shapes exactly at the filling transition temperature.* For this case the temperature T is tuned exactly to the filling transition of the fluid on the (infinite) A-wedge, i.e. the temperature satisfies $\theta_A(T_F) = \alpha$. This is the marginal value of the temperature at which the maximum droplet height ℓ_0^{max} becomes macroscopic as $L \to \infty$.

(B) *Droplet shapes above the filling transition temperature.* If $T > T_F$, then the droplet height also grows to infinity as $L \to \infty$. However, because of the relevance of the linear term in the filling binding potential (50), we cannot assume that the scaling of the droplet shape is the same as that obtained exactly at $T = T_F$. Indeed droplet shapes for $T > T_F$ may be viewed as finite-size effects occurring at the complete-filling transition. However, fluctuations here do not have the same quasi-one-dimensional characteristics as critical filling. Analysis of the critical exponents at complete filling shows that ξ_x and ξ_y diverge with the same critical exponent as $\mu \to \mu_{sat}^-(T)$ [9, 10]. Consequently the 1D model

(49) is not justified for this transition and analysis of the droplet shape in the present heterogeneous wedge problem must be based on the full model (47). This is a much more difficult problem and we will not consider this here.

Our treatment of droplet shapes in the wedge parallels that of droplet shapes on planar substrates. The effective Hamiltonian on the heterogeneous wedge is taken to be the generalization of the filling model (49):

$$H_F[\ell_0] = \int \mathrm{d}y \left\{ \frac{\Sigma \ell_0}{\alpha} \left(\frac{\mathrm{d}\ell_0}{\mathrm{d}y} \right)^2 + V(\ell_0; y) \right\} \tag{55}$$

where $V(\ell_0; y)$ is a position-dependent direct filling potential that changes from being of type $V_A(\ell_0)$ to being of type $V_B(\ell_0)$ as one crosses the heterogeneous region. The Ward identity for this model is again easily derived. We find

$$\frac{2\Sigma}{\alpha} \langle \ell_0(y) \ell_0''(y) \rangle = \left\langle \frac{\partial V'}{\partial \ell_0}(\ell_0; y) \right\rangle + \frac{\Sigma}{\alpha} \left\langle \ell_0'(y)^2 \right\rangle \tag{56}$$

so for within the droplet we can write

$$\frac{2\Sigma}{\alpha} \langle \ell_0(y) \ell_0''(y) \rangle - \frac{\Sigma}{\alpha} \langle \ell_0'(y)^2 \rangle = \langle V_A'(\ell_0) \rangle. \tag{57}$$

To evaluate the RHS we again resort to the concept of an effective potential, which we showed to yield exact results for the wetting droplet in 1 + 1 dimensions. Thus we seek to solve the field equation (writing $\langle \ell_0 \rangle \equiv \ell_0$, for convenience)

$$\frac{2\Sigma}{\alpha} \ell_0 \ell_0'' + \frac{\Sigma}{\alpha} \ell_0'^2 = V_{eff}'(\ell_0) \tag{58}$$

using the effective potential V_{eff} evaluated at $T = T_F$ for short-ranged and long-ranged forces. For long-ranged forces we will assume that $p = 2$ as is appropriate for realistic solid–fluid interfaces. This differential equation is easily integrated using standard techniques and we only quote the final results.

For droplet scaling exactly at T_F and short-ranged forces, we find

$$\langle \ell_0(y) \rangle = \ell_0^{max} 4^{1/3} \left[\frac{y}{L} \left(1 - \frac{y}{L} \right) \right]^{1/3} \tag{59}$$

where $\ell_0^{max} \propto L^{1/3}$ denotes the mid-drop height. Note that this scaling form is precisely in accord with the prediction of conformal invariance for one-dimensional interfaces with wandering exponent $\zeta = 1/3$. For long-ranged forces, on the other hand, integration of (58) yields a quite different form of the scaling function. We find that $\langle \ell_0(y) \rangle / \ell_0^{max} \equiv \tilde{\ell}_0(y)$ satisfies the cubic equation

$$3\tilde{\ell}_0^2 + \tilde{\ell}_0^3 = 16 \frac{y}{L} \left(1 - \frac{y}{L} \right) \tag{60}$$

with $\ell_0^{max} \sim L^{1/2}$. Thus the scaling of droplet shapes at wedge wetting is only consistent with conformal invariance for systems with short-ranged forces. Equations (59) and (60) are the main new predictions of this section and are explicit predictions for the scaling of the droplet shape in wedge geometries at the filling temperature. Again these expressions are valid in the scaling limit of large L and distances y that are many bulk correlation lengths away from the edge of the drop.

4. Conclusion

In this paper we have investigated the scaling behaviour of finite-size droplet shapes on heterogeneous planar substrates and wedges. Our predictions are restricted to systems at two-phase bulk liquid–vapour coexistence (chemical potential $\mu = \mu_{sat}$) in the grand canonical ensemble, i.e. without volume constraint. The main conclusions of this article are the following:

(A) For three-dimensional systems with short-ranged forces the scaling of the droplet shape and its height–height correlations can be understood using conformal invariance. In fact using standard wetting renormalization group ideas the conformal invariance may be explicitly proved for such systems. Consequently the study of droplet shapes in laboratory systems with effective short-ranged forces such as polymers, superconductors, liquid metals and even some fluid–fluid interfaces may be viewed as a possible experimental testing ground for many of the ideas developed in conformal-field theory as well of course as the fluctuation theory of fluid interfaces.

(B) For three-dimensional systems with long-ranged (van der Waals) dispersion forces the droplet shape still exhibits a strong degree of scaling-invariance-related behaviour even though there is no longer any conformal invariance.

(C) For model systems of interfaces in two-dimensional bulk geometries with short-ranged forces the scaling shape of the droplet on the heterogeneous wall can be understood quantitatively using an effective potential accounting for the entropic repulsion of the interface from the wall and is completely in accord with the predictions of conformal invariance for one-dimensional field theories.

(D) Finite-size droplets in wedge geometries show a number of interesting scaling behaviours depending on whether the interfacial pinning is done exactly at or above the filling transition temperature. Exactly at T_F and for systems with short-ranged forces the prediction of conformal invariance for the shape function is again valid. For long-ranged forces a different scaling behaviour is observed.

The predictions of this paper are based entirely on the analysis of effective interfacial models. It would be interesting to test these ideas using more microscopic approaches such as density-functional theory. The density (or magnetization) profile for such systems is of course highly inhomogeneous and even analysis of a Landau-like model would require numerical methods. Beyond the mean-field level, Ising model simulations could test the role of the wetting parameter in determining the scale of the droplet height. Finally we hope that at least some of our predictions are open to experimental verification from observation of droplet shapes in the micrometre range.

Acknowledgments

E D Macdonald acknowledges the EPRSC for a studentship and CR acknowledges the financial assistance of the EC under contract ERBFMBICT983229.

Appendix

We show here that, in two dimensions, the equation

$$\nabla^2 \ell = C\mathrm{e}^{-\tilde{\kappa}\ell} \tag{A.1}$$

(where C and $\tilde{\kappa}$ are real numbers) is conformally invariant. In particular, we demonstrate that equation (A.1) is invariant under the following conformal transformations:

$$\begin{aligned}&(x, y) \longrightarrow (u, v)\\ &\mathrm{e}^{-\tilde{\kappa}\ell(x,y)} \longrightarrow \mathrm{e}^{-\tilde{\kappa}\overline{\ell}(u,v)}|w'|^{x_b}\end{aligned} \tag{A.2}$$

where (u, v) are given by the relation (in the complex plane) $u + \mathrm{i}v = w(z)$, $z \equiv x + \mathrm{i}y$, $w(z)$ is any analytic function, $|w'|$ is the local length rescaling factor of the transformation and $x_b = 2$.

If we define

$$\nabla \equiv \left(\frac{\partial}{\partial x}, \frac{\partial}{\partial y}\right)$$

$$\overline{\nabla} \equiv \left(\frac{\partial}{\partial u}, \frac{\partial}{\partial v}\right)$$

$$J \equiv |w'(z)|^2 = \left(\frac{\partial u}{\partial x}\right)^2 + \left(\frac{\partial v}{\partial x}\right)^2$$

substitution of (A.2) into (A.1) yields

$$\nabla^2\overline{\ell} - \frac{x_b}{2\tilde{\kappa}}\nabla^2 \log J = C\mathrm{e}^{-\tilde{\kappa}\overline{\ell}(u,v)} J^{x_b/2}. \tag{A.3}$$

Using analytic properties of the conformal transformation

$$\frac{\partial u}{\partial x} = \frac{\partial v}{\partial y} \qquad \frac{\partial u}{\partial y} = -\frac{\partial v}{\partial x}$$

and standard methods, it can be shown that $\nabla^2 \log J = 0$ and $\nabla^2 = J\overline{\nabla}^2$. Therefore, equation (A.3) transforms into

$$J\,\overline{\nabla}^2\overline{\ell} = C\mathrm{e}^{-\tilde{\kappa}\overline{\ell}(u,v)} J^{x_b/2}$$

which, in turn, recovers (A.1) for $x_b = 2$.

References

[1] Lenz P and Lipowsky R 1998 *Phys. Rev. Lett.* **80** 1920
[2] Gau H, Herminghaus S, Lenz P and Lipowsky R 1999 *Science* **283** 46
[3] Swain P S and Lipowsky R 1998 *Langmuir* **14** 6772
[4] Bauer C, Dietrich S and Parry A O 1999 *Europhys. Lett.* **47** 474
[5] Bauer C and Dietrich S 1999 *Phys. Rev.* E **60** 6919
[6] Rascón C, Parry A O and Sartori A 1999 *Phys. Rev.* E **59** 5697
[7] Rascón C and Parry A O 1998 *Phys. Rev. Lett.* **81** 1267
[8] Rascón C and Parry A O 2000 *J. Chem. Phys.* **112** 5175
[9] Parry A O, Rascón C and Wood A J 1999 *Phys. Rev. Lett.* **83** 5535
[10] Parry A O, Rascón C and Wood A J 1999 *Phys. Rev. Lett.* **85** 345
[11] Fisher M E and de Gennes P-G 1978 *C. R. Acad. Sci., Paris* B **287** 207
[12] Krech M 1994 *The Casimir Effect in Critical Systems* (Singapore: World Scientific)
[13] Mikheev L V and Weeks J D 1991 *Physica* A **177** 495
[14] Parry A O and Evans R 1993 *Mol. Phys.* **78** 1527
[15] Brézin E, Halperin B I and Leibler S 1983 *Phys. Rev. Lett.* **50** 1387
[16] Fisher D S and Huse D A 1985 *Phys. Rev.* B **32** 247
[17] Lipowsky R and Fisher M E 1987 *Phys. Rev.* B **36** 2126
[18] Schick M 1990 *Liquids at Interfaces (Les Houches, Session XLVIII)* ed J Charvolin, J F Joanny and J Zinn-Justin (Amsterdam: North-Holland)
[19] Forgacs G, Lipowsky R and Nieuwenhuizen Th M 1991 *Phase Transitions and Critical Phenomena* vol 14, ed C Domb and J L Lebowitz (London: Academic)

[20] Kerle T, Klein J and Binder K 1996 *Phys. Rev. Lett.* **77** 1318
[21] Ross D, Bonn D and Meunier J 1999 *Nature* **400** 737
[22] Indekeu J O and van Leeuwen J M J 1995 *Phys. Rev. Lett.* **75** 1618
[23] Fisher M E and Wen H 1992 *Phys. Rev. Lett.* **68** 3654
[24] Evans R, Hoyle D C and Parry A O 1992 *Phys. Rev.* A **45** 3823
[25] Cardy J L 1987 *Phase Transitions and Critical Phenomena* vol 11, ed C Domb and J L Lebowitz (London: Academic)
[26] Burkhardt T W and Eisenriegler E 1985 *J. Phys. A: Math. Gen.* **18** L83
[27] Binder K, Landau D P and Kroll D M 1986 *Phys. Rev. Lett.* **56** 2272
[28] Binder K, Landau D P and Ferrenberg A M 1995 *Phys. Rev. Lett.* **74** 298
[29] Boulter C J and Parry A O 1995 *Phys. Rev. Lett.* **74** 3403
[30] Parry A O, Boulter C J and Swain P S 1995 *Phys. Rev.* E **52** R5768
[31] Parry A O and Evans R 1990 *Phys. Rev. Lett.* **64** 439
[32] Cardy J L 1984 *Nucl. Phys.* B **240** 514
[33] Diehl H W 1986 *Phase Transitions and Critical Phenomena* vol 10, ed C Domb and J L Lebowitz (London: Academic)
[34] Borjan Z and Upton P J 1998 *Phys. Rev. Lett.* **81** 4911
[35] Parry A O, Macdonald E D and Rascón C 2001 to appear
[36] Parry A O and Swain P S 1997 *J. Phys.: Condens. Matter* **9** 2351
[37] Lipowsky R 1984 *Phys. Rev. Lett.* **52** 1429
[38] Burkhardt T W 1989 *Phys. Rev.* B **40** 6987
[39] Concus P and Finn R 1969 *Proc. Natl Acad. Sci. USA* **63** 292
[40] Pomeau Y 1986 *J. Colloid Interface Sci.* **113**
[41] Hauge E H 1992 *Phys. Rev.* A **46** 4994
[42] Rejmer K, Dietrich S and Napiórkowski M 1999 *Phys. Rev.* E **60** 4027